



## Anti-Endoglin monoclonal antibody prevents the progression of liver sinusoidal endothelial inflammation and fibrosis in MASH

Samira Eissazadeh <sup>a,1</sup>, Petra Fikrova <sup>a,1</sup>, Jana Urbankova Rathouska <sup>a</sup>, Ivana Nemeckova <sup>a</sup>, Katarina Tripska <sup>a</sup>, Martina Vasinova <sup>a</sup>, Radim Havelek <sup>b</sup>, SeyedehNiloufar Mohammadi <sup>a</sup>, Ivone Cristina Igreja Sa <sup>a,c</sup>, Charles Theuer <sup>d</sup>, Matthias König <sup>e</sup>, Stanislav Micuda <sup>f</sup>, Petr Nachtigal <sup>a,\*</sup>

<sup>a</sup> Department of Biological and Medical Sciences, Faculty of Pharmacy in Hradec Kralove, Charles University, Hradec Kralove, Czech Republic

<sup>b</sup> Department of Biochemistry, Faculty of Medicine in Hradec Kralove, Charles University, Hradec Kralove, Czech Republic

<sup>c</sup> Department of Clinical Microbiology, Faculty of Medicine in Hradec Kralove, Charles University, Hradec Kralove, Czech Republic

<sup>d</sup> Tacon Pharmaceuticals, Inc., San Diego, CA, United States

<sup>e</sup> Institute for Theoretical Biology, Institute for Biology, Systems Medicine of the Liver, Humboldt University Berlin, Germany

<sup>f</sup> Department of Pharmacology, Faculty of Medicine in Hradec Kralove, Charles University, Hradec Kralove, Czech Republic

### ARTICLE INFO

#### Keywords:

Liver sinusoidal endothelial inflammation

Endoglin

Anti-endoglin antibody

Fibrosis

Liver alteration

### ABSTRACT

Liver sinusoidal endothelial inflammation/dysfunction and fibrosis are a crucial part of Metabolic Dysfunction Associated Steatohepatitis (MASH) development. TRC105 and M1043 are anti-endoglin (ENG) monoclonal antibodies that bind ENG. In this study, we hypothesized that treatment with anti-ENG antibodies would prevent the progression of LSECs inflammation and fibrosis *in vivo* and *in vitro*.

MASH was induced in male C57BL/6 mice fed a choline-deficient L-amino acid-defined high-fat diet (CDAA-HFD) for 4 or 8 weeks. In the rescue study, mice were divided into three groups: a control group (chow diet), a MASH group (CDAA-HFD + IgG), and a rescue group (CDAA-HFD + M1043). Later, two groups received rat IgG1 (10 mg/kg) and M1043 (10 mg/kg). In *in vitro* experiments, inflammation was induced in human LSECs by ox-LDL (50 µg/mL) and treated with TRC105 (300 µg/mL).

Liver sinusoidal endothelial inflammation/dysfunction in MASH animals was characterized by endothelial overexpression of ENG, VCAM-1, and ICAM-1 and reduced VE-cadherin and p-eNOS/eNOS expression. M1043 treatment prevented the overexpression of ENG, VCAM-1, and ICAM-1, the progression of liver fibrosis, and the increase of liver-to-body weight ratio. *In vitro* experiments with TRC105 confirmed the prevention of LSECs inflammation development by reduced ENG and VCAM-1 expression, as well as decreased THP-1 monocytic cell adhesion in ox-LDL activated LSECs.

In conclusion, we demonstrate that anti-ENG antibody treatment can prevent LSECs inflammation and fibrosis progression in a MASH animal model and LSECs inflammation *in vitro*. Thus, we propose directly targeted ENG may represent a promising pharmacological approach for addressing LSECs inflammation and liver fibrosis.

### 1. Introduction

Metabolic Dysfunction-Associated Steatohepatitis (MASH (previously known as non-alcoholic steatohepatitis (NASH)), an advanced form of Metabolic Dysfunction Associated Fatty Liver Disease (MAFLD (the previous term was non-alcoholic fatty liver disease (NAFLD)), is a

rapidly growing health problem where reliable therapy is still not available, which leads to liver cancer and transplantation. Therefore, understanding the molecular mechanisms behind this disease and developing effective medications is critically important. Liver sinusoidal endothelial cells (LSECs), which encompass the most permeable endothelium in the liver, are highly specialized endothelial cells that form the

\* Corresponding author at: Department of Biological and Medical Sciences, Faculty of Pharmacy in Hradec Kralove, Charles University, Heyrovského 1203, Hradec Kralove 500 05, Czech Republic.

E-mail address: [petr.nachtigal@faf.cuni.cz](mailto:petr.nachtigal@faf.cuni.cz) (P. Nachtigal).

<sup>1</sup> These authors contributed equally to the manuscript

fenestrated walls of the hepatic sinusoids and represent about 15 %–20 % of liver cells despite occupying only 3 % of the total hepatic volume. They regulate the transfer of molecules and cells between the liver parenchyma and the blood [1]. LSECs exhibit anti-inflammatory and anti-fibrogenic properties by inhibiting the activation of Kupffer cells and hepatic stellate cells (HSCs) and regulating intrahepatic vascular resistance and portal pressure [2,3]. During acute or chronic liver injury, LSECs undergo phenotypic changes (resulting in capillarization), negatively affecting their protective properties and leading to liver sinusoidal endothelial dysfunction (LSED). Indeed, LSED is represented by increased expression of cell adhesion molecules, defective vasodilation, and endothelial inflammation [2–5]. These changes activate neighboring HSCs and promote their differentiation into a profibrotic phenotype, which is the crucial step from steatosis to fibrosis and the development of MASH [6].

Our previous papers showed that endoglin (ENG), a co-receptor of transforming growth factor  $\beta$ , plays an interesting role in liver pathologies, including MASH [7,8]. ENG, in the liver predominantly expressed in LSECs near the central vein, has been shown to be essential for maintaining endothelial function in LSECs through balanced physiological expression in the intrahepatic cholestasis and MASH mouse model [7]. In addition, it has been demonstrated recently that ENG appears to be a crucial molecule in the development of endothelial dysfunction (ED), as well as in the adhesion and transmigration of monocytes through the endothelium [7,9,10]. Moreover, soluble endoglin (sENG) is the form of ENG that is cleaved and released into the bloodstream from the membrane-bound form of ENG, and it has been proposed as a biomarker of liver injury, including intrahepatic cholestasis and MASH [7].

Indeed, having the tool to modulate ENG and its signaling to influence the progression of MASH would be highly valuable. Interestingly, TRC105 or carotuximab (chimeric human IgG1) is a human therapeutic monoclonal antibody (mAb) that can bind human ENG with high avidity and inhibits BMP-9 binding [11]. It has been studied in several clinical trials in oncology and age-related macular degeneration [12–14]. It was demonstrated that TRC105 blocked ENG, resulting in the prevention of hypercholesterolemia and hyperglycemia-induced ED in human aortic endothelial cells [8,10]. TRC105 has a lower affinity to mouse ENG, resulting in less significant inhibition. Thus, a mouse-specific ENG-targeting rat IgG1 antibody, M1043, has been formulated for a specific application in preclinical studies, and this antibody efficiently inhibits BMP-9-induced signaling in mice [11].

It is worth mentioning that the BMP-9 signaling pathway activates the downstream effector inhibitor of differentiation or DNA binding 1 (ID1), which we studied in the context of ENG blockage. ID1 is a member of the helix-loop-helix family of transcription factors that regulate angiogenesis and inflammation. Interestingly, BMP-9/SMAD1/5/ID1 signaling has been shown to be responsible for the transdifferentiation of HSCs into myofibroblasts, a process crucial for liver fibrogenesis [15]. In addition, ID1 expression leads to the upregulation of NF- $\kappa$ B activity, suggesting a critical role in inflammation [16].

Liver inflammation involves leukocyte transmigration, a well-organized, multistep process that includes rolling the leukocytes on the endothelium, activation, firm adhesion to the endothelial wall, intravascular crawling, and finally, transmigration into the tissue. Vascular Cell Adhesion Molecule-1 (VCAM-1) and Intercellular Cell Adhesion Molecule-1 (ICAM-1) are highly expressed in inflamed LSECs and are essential for leukocyte transmigration into the inflamed liver tissue [17]. Both VCAM-1 and ICAM-1 were shown to participate in liver sinusoidal endothelial inflammation development. VCAM-1 has been identified as a mediator of monocyte adhesion to LSECs. In addition, it was demonstrated that VCAM-1 was expressed by LSECs, promoting capillarization during liver impairment and exhibiting a profibrogenic role in liver fibrosis [18]. Moreover, we showed that VCAM-1 is predominantly expressed by LSECs in our previous paper [7]. Interestingly, ICAM-1 was strongly and predominantly expressed by LSECs in our

previous paper [7]. It has been established that blocking ICAM-1 in LSECs reduces the adhesion and transmigration of tumor cells through LSECs both *in vitro* and *in vivo* [19]. Similarly, ENG has been shown to be involved in leucocyte adhesion and transmigration during inflammation through its interaction, at least with the activated integrin  $\alpha 5\beta 1$  [9].

In addition to biomarkers of sinusoidal inflammation associated with LSED, there are other biomarkers characterizing LSED, including Vascular Endothelial Cadherin (VE-cadherin) and endothelial Nitric Oxide Synthase (eNOS). VE-cadherin regulates processes in blood vessel formation and plays a key role in endothelial cell-to-cell adherent junctions to maintain vascular integrity, control vascular permeability, and restrain vascular growth by maintaining endothelial cell junctions and stabilizing the endothelial monolayer [20]. Moreover, reduced VE-cadherin disrupts the adherent junctions in LSECs, leading to LSED characterized by increased permeability and loss of selective barrier function. eNOS activity plays an important role in regulating endothelial function and vascular tone through the production of nitric oxide (NO) [21]. NO produced by activated eNOS regulates the permeability of the endothelial layer, preventing excessive leakage of plasma components into the liver parenchyma. In liver diseases such as cirrhosis and MAFLD, eNOS activity and NO production are often impaired. This promotes the expression of adhesion molecules and the recruitment of inflammatory cells, exacerbating LSED [22].

Our previous findings emphasized the importance of maintaining the physiological expression of ENG for the proper function of LSECs *in vivo* [7]. In addition, we showed the crucial impact of possible ENG blocking in aortic endothelial cells with respect to the progression of ED and adhesion and transmigration of monocytes *in vitro* [10,23]. Thus, we hypothesized that anti-ENG antibody treatment would prevent the progression of LSECs inflammation and fibrosis *in vivo* (during MASH progression) and *in vitro*.

## 2. Methods and materials

### 2.1. *In vivo* experimental design

The 10-week-old male C57BL/6J mice were used in this study and were purchased from Velaz company (Prague, Czech Republic). After two weeks of acclimation, and during the study, the animals were kept in a temperature-controlled room ( $22^{\circ}\text{C} \pm 1^{\circ}\text{C}$ ) with a 12-h light/dark cycle and constant humidity. The mice had free access to drinking water and *ad libitum* rodent diets throughout the study.

The main study was conducted in two separate parts. In the first phase, we studied disease progression by inducing MASH in two groups of mice ( $n = 7$ ) by feeding them a CDAA-HFD (Choline-Deficient, L-Amino Acid-Defined, High-Fat Diet With 60 kcal% Fat With 0.1 % Methionine and No Added Choline) (A06071302, Research Diets, New Brunswick, NJ, USA) for either four or eight weeks. Age-matched control groups ( $n = 7$ ) were fed a standard chow diet (1314–10 mm pellets, Altromin, Lage, NRW, Germany). Subsequently, the mice were euthanized by anesthetic overdose induced by a combination of xylazine (10 mg/kg, i.p.) and ketamine (100 mg/kg, i.p.), followed by blood collection from the *inferior vena cava* for biochemical analysis and harvesting of the liver for molecular analysis.

In the second part of the study (a rescue study to prove the concept), twenty-four mice were divided into three groups: a control group ( $n = 8$ ) fed a chow diet for 8 weeks, a MASH-diet induced group fed CDAA-HFD + IgG ( $n = 8$ ), and a rescue study group fed CDAA-HFD + M1043 ( $n = 8$ ), the mAb anti-ENG. After a four-week period of feeding, during which MASH development was confirmed in the initial study, both CDAA-HFD-fed groups received intraperitoneal (i.p.) injections of either rat IgG1 (TRACON Pharmaceuticals Inc., San Diego, CA, USA) (10 mg/kg body weight) or M1043 (TRACON Pharmaceuticals Inc., San Diego, CA, USA) (10 mg/kg body weight) twice weekly for an additional four weeks. Upon completion of the 8-week experimental period, mice were euthanized using the same anesthesia overdose method, and blood from the

*inferior vena cava*, as well as liver samples, were harvested for further analysis.

The number of individuals in each group was determined using Power analysis with the G\*Power program, based on the following parameters: statistical evaluation utilized a non-parametric Mann-Whitney test between two independent groups, with  $\alpha$  set at the 0.05 significance level. In addition, we followed the 3Rs and the Five Freedom Principles for animal welfare [24], resulting in a reduced sample size of 7 (during the progression study) and 8 (during drug administration study) mice per group in each phase of the study. This adjustment was necessary due to the increased risk of mortality and variability in liver damage parameters caused by induction of liver impairment via CDAA-HFD and the administration of rat IgG1 and M1043.

All animals were taken care of in accordance with the guidelines set by the Charles University Ethical Committee, Faculty of Pharmacy in Hradec Kralove, to ensure the welfare of laboratory animals (Project number MSMT- 5793/2021-2, approval date: 4 May 2021). All planned experiments were carried out in accordance with Czech Law No. 246/1992 Sb. In addition, the utilization of experimental animals and the research protocol have been registered and approved successfully by the board of the International Register of Preclinical Trial Protocols (<http://preclinicaltrials.eu>) under registration number PCTE00000526.

## 2.2. *In vitro* experimental design

An *in vitro* study was conducted to investigate the mechanistic basis of LSECs inflammation markers changes and to confirm the therapeutic efficacy of a mAb targeted ENG blockade observed in an animal model of MASH. To achieve this goal, Human Hepatic Sinusoidal Endothelial Cells (HHSECs, hereafter referred to as LSECs) were treated with the anti-human ENG mAb TRC105 (TRACON Pharmaceuticals Inc., San Diego, CA, USA) to determine whether LSECs could be responsible for effects observed in *in vivo* study.

LSECs were purchased from Innoprot company (P10652, Derio, Bizkaia, Spain). The cells were cultured in the gelatin-coated flask in an endothelial cell medium (P60104, Innoprot, Derio, Bizkaia, Spain) with corresponding supplements at 37 °C and 5 % CO<sub>2</sub>. Cells were passaged after reaching 70–90 % confluence, and all experiments were performed with LSECs passage five. To study LSEC-specific ENG blockade effects observed *in vivo*, LSECs inflammation has been induced *in vitro* by Oxidized Low-Density Lipoprotein (ox-LDL) (L34357, Thermo Fisher Scientific, Waltham, MA, USA). Cells were treated with ox-LDL (50 µg/mL) for 48 h to assess protein expression of ENG and cell adhesion molecules (VCAM-1, ICAM-1) by multicolor flow cytometry (median fluorescence intensity: MFI) and cell adhesion of THP-1 monocytic cells. A rescue study was performed by pre-treatment of LSECs with TRC105 (300 µg/mL) for 3 h prior to the addition of ox-LDL. For the control group, LSECs underwent the same experimental conditions and media exchange procedure as the treatment groups but without receiving any treatment intervention. The concentration and time of ox-LDL and TRC105 were chosen based on preliminary experiments and previously published studies [25]. To assess the immediate effect of ENG blockage in ox-LDL-induced LSECs inflammation, a shorter incubation time of 16 h was chosen for the assessment of sENG, while a 6-h incubation period was selected for the evaluation of mRNA levels of *ENG*, *VCAM-1*, *ICAM-1* and *ENG* transcription factors expression using quantitative real-time RT-PCR.

The human acute monocytic leukemia cell line (THP-1) (88,081,201, European Collection of Cell Culture, Salisbury, Wiltshire, UK) cells were cultured in RPMI 1640 medium (11,875,093, Thermo Fisher Scientific, Waltham, MA, USA) supplemented with 10 % fetal bovine serum (FBS) (Biosera, Cholet, France), 1 % penicillin-streptomycin (P0781, MilliporeSigma, Burlington, MA, USA), and 2.5 % glutamine (Thermo Fisher Scientific, Waltham, MA, USA). THP-1 cells were passaged when density  $8 \times 10^5$  cells/mL was reached, and all experiments were conducted with cells up to passage twenty-five.

## 2.3. Biochemical assays

Fresh blood (100 µL) was applied to the Preventive Care Profile Plus cartridge test (Abaxis, Griesheim, Hesse, Germany) for the measurement of liver enzymes and total bilirubin using the VetScan2 device (Abaxis, Griesheim, Hesse, Germany).

## 2.4. Quantitative real-time RT-PCR

The expression of mRNA was evaluated by real-time quantitative reverse transcription-polymerase chain reaction (qRT-PCR) in the QuantStudio 6 Flex Real-Time PCR Software in duplicates (Applied Biosystems, Thermo Fisher Scientific, MA, USA), as previously described [32]. For the normalization of the data, the mouse Glyceraldehyde 3-phosphate dehydrogenase (*Gapdh*) and human *GAPDH* genes were used as references for *in vivo* and *in vitro* experiments, respectively. Supplementary Data 1, Table 1 indicates the primers used for the analysis.

## 2.5. Western blot analysis

The total and membrane fractions of the liver were prepared from liver homogenates as previously described [25]. SDS-PAGE separated homogenates on 6 %, 8 %, 10 %, and 12 % polyacrylamide gels according to the molecular weight of the desired proteins and then transferred to nitrocellulose membranes (Bio-Rad Laboratories, Hercules, CA, USA). Subsequently, the membranes were blocked for 1 to 1.5 h with 5 % non-fat dry milk Bio-Rad Laboratories, Hercules, CA, USA) in Tris-Buffered Saline containing 0.1 % Tween 20 (MilliporeSigma, Burlington, MA, USA) (TBS-T), and then incubated overnight at 4 °C with primary antibodies at suitable concentrations (see Supplementary Data 1, Table 2). The membranes were washed six times with TBS-T and then incubated for an hour at room temperature on a shaker with the appropriate HRP-conjugated secondary antibodies (see Supplementary Data 1, Table 2), followed by another round of washing with TBS-T. The protein bands were visualized using the ChemiDoc™ MP Imaging System (Bio-Rad Laboratories, Hercules, CA, USA). Image Lab software (version 6.1, Bio-Rad Laboratories, Hercules, CA, USA) was used for band quantification. The expression levels of proteins were normalized according to Ponceau S (Serva Electrophoresis GmbH, Heidelberg, Germany) staining.

## 2.6. Multicolor immunofluorescence flow cytometry

LSECs were seeded in gelatin-coated plates according to the study design, followed by washing with phosphate-buffered saline (PBS) (MilliporeSigma, Burlington, MA, USA) and then detached using Accutase™ (Thermo Fisher Scientific, Waltham, MA, USA). Multicolor flow cytometry was used to assess the surface expression of ENG, VCAM-1, and ICAM-1. Cells were blocked and rinsed with PBS containing 2 % FBS. Subsequently, the cells were incubated with specific fluorophore-conjugated antibodies (see Supplementary Data 1, Table 3) for 30 min at 4 °C in the dark. After incubation, the cells were rinsed again with PBS containing 2 % FBS, and then the cell pellet was resuspended in PBS. Protein expression was evaluated using a Cytoflex LX Flow Cytometer (Beckman Coulter, Brea, CA, USA) and analyzed with CytExpert Acquisition and Analysis Software, version 2.3 (Beckman Coulter, Brea, CA, USA). For each sample, a minimum of 10,000 events were collected and analyzed, and the level of MFI was measured and evaluated.

## 2.7. Cell adhesion assays

LSECs were seeded in gelatin-coated plates and treated according to the study design. Afterward, THP-1 monocytic cells pre-labeled with Vybrant-Dio (4 µL/1 million of THP-1, 15 min) were added to LSECs monolayers for 1 h. Non-adherent cells were removed by washing the

12-well plates with PBS. LSECs with adherent THP-1 cells were detached with Accutase™. The Vybrant-Dio positive cells (in combination with side and forward scatter) were quantified as adherent THP-1 cells using a flow cytometer.

#### 2.8. sENG protein analysis in mouse plasma and cell culture media

The plasma levels of mouse sENG during the first phase of the *in vivo* study were measured using the Mouse Endoglin/CD105 Quantikine ELISA Kit (MNDG00, R&D Systems, MN, USA), following the manufacturer's instructions, with measurements performed in duplicate. However, in both *in vivo* and *in vitro* rescue studies, to avoid undesirable cross-reactions between detection antibodies and the ENG-blocking mAbs (M1043 and TRC105), the method was switched from ELISA to western blot analysis, a semi-quantitative method.

This change was necessary because the ENG-blocking mAbs could interfere with antibody detection in ELISA assays, resulting in inaccurate sENG measurement. Western blotting, being less prone to such cross-reactivity, offered a more specific and reliable approach for detecting sENG levels in mouse plasma and cell culture media.

To ensure sufficient protein content for accurate detection, plasma and culture media samples were concentrated before western blot analysis. 100 µL of each sample was transferred to a centrifuge tube and placed in a Vacufuge Concentrator 5301 (Eppendorf, Hamburg, Germany) set at room temperature for 25 min, followed by an additional round at 30 °C for another 25 min for mouse plasma and 45 min for media. The protein concentration of the samples was measured, and afterward, western blot analysis was performed to compare the levels of sENG protein among different groups in the mouse plasma and culture media. The control group was normalized to 100 % for comparison.

#### 2.9. Histological analysis

Liver sections were fixed in 4 % paraformaldehyde, followed by embedding liver sections in paraffin. Serial cross-sections (4.5 µm of thickness) were cut and stained with the Sirius Red/Fast Green Collagen Staining Kit (9046, Chondrex, WA, USA) for histological analysis. Microscopic pictures were captured by an Olympus AX 70 microscope with an incorporated Nikon DS-Fi3 high-definition colour microscope camera and image analysis software NIS (Laboratory Imaging, Czech Republic). For the Sirius Red/Fast Green Collagen quantification, 4 mice from CDAA-HFD 4, 8 weeks groups, CDAA-HFD + IgG, and CDAA-HFD + M1043 groups were used. Twenty sections from each liver were cut, and systematic uniform random sampling [26] was used to choose 4 sections from each liver for the quantification by Image Analysis software NIS. The results are presented as the percentage of area of Sirius Red/Fast Green Collagen positivity per section.

#### 2.10. Statistical analysis

The statistical analysis was performed using GraphPad Prism software version 10 (GraphPad Software Inc., San Diego, CA, USA). Data are presented as median with interquartile range. Group-group comparisons were conducted using the non-parametric Mann-Whitney test. *P*-values <0.05 were considered statistically significant.

### 3. Results

#### 3.1. CDAA-HFD induces liver injury

Although there was a decrease in body weight (Fig. 1A) in both the 4-week and 8-week CDAA-HFD-fed mice compared to their respective control groups, no significant difference in body weight was observed between the 4-week and 8-week MASH mice. Both the 4-week and 8-week MASH groups showed a significant increase in liver weight (Fig. 1B) and the liver-to-body weight ratio (Fig. 1C) compared to their

respective control groups, suggesting liver hepatomegaly in both MASH groups. Interestingly, the liver-to-body weight ratio was significantly higher in the 8-week MASH mice compared to the 4-week MASH mice, suggesting a time-dependent progression of liver impairment.

Additionally, significant elevations were observed in the activity of alanine transaminase (ALT) (Fig. 1D), aspartate aminotransferase (AST) (Fig. 1E), and total bilirubin concentration in plasma (Fig. 1F) in both the 4-week and 8-week mouse models of MASH compared to their respective control groups, confirming liver injury induced by CDAA-HFD.

Notably, total bilirubin levels were significantly higher in the 8-week CDAA-HFD group compared to the 4-week MASH animals, indicating mild progression of liver alteration after 8 weeks of feeding with CDAA-HFD.

#### 3.2. MASH diet induces LSECs inflammation and increases sENG levels

The protein expression of ENG (Fig. 2A) and sENG levels (Fig. 2B) showed a significant increase in both the 4-week and 8-week mice compared to their respective control groups. Furthermore, plasma sENG levels in the 8-week MASH animals were significantly elevated compared to the 4-week MASH animals, which might be related to the upregulated hepatic protein expression of ENG in the 8-week MASH mice compared to the 4-week MASH mice, suggesting a worsening of LSECs inflammation. Immunohistochemical analysis (IHC) confirmed the western blot results and showed ENG positivity primarily in LSECs near the central vein (Supplementary Data 2).

Interestingly, ENG was not detected in hepatocytes or cholangiocytes and was very weak in endothelial cells in arterioles and venules in the portal triad area (Supplementary Data 2).

VCAM-1 (Fig. 2C) and ICAM-1 (Fig. 2D) protein expressions were significantly increased in both 4- and 8-week MASH mice compared to their respective control groups. In addition, both VCAM-1 and ICAM-1 protein expressions were significantly upregulated in 8-week MASH animals, demonstrating aggravation of LSECs inflammation. In addition, IHC analysis of VCAM-1 followed its protein expression profile (Supplementary Data 2). The CDAA-HFD significantly increased VCAM-1 protein expression, predominantly in LSECs in MASH mice. Although western blot analysis showed a significant increase in ICAM-1 in MASH mice and an upregulation from 4 weeks to 8 weeks, the staining intensity and pattern of ICAM-1 were similar across all groups. IHC analysis revealed that ICAM-1 expression was mostly detected in endothelial cells in sinusoids, the central vein, portal triad venules, and arterioles area (Supplementary Data 2).

Furthermore, protein expressions of VE-cadherin (Fig. 2E) and p-eNOS/eNOS (Fig. 2F) showed a significant reduction in both MASH animal groups, supporting LSED development in all MASH mice. However, the expression of VE-cadherin and p-eNOS/eNOS proteins in 8-week mice did not reach statistical significance when compared to the 4-week MASH animals, indicating that continued progression of MASH in our mouse model does not result in further downregulation of VE-cadherin and p-eNOS/eNOS protein expression.

#### 3.3. MASH diet induces liver fibrosis

While a significant increase in the liver protein expression of alpha-smooth muscle actin ( $\alpha$ -SMA) (Fig. 3A) was observed in both MASH groups compared to their respective control groups, the expression of  $\alpha$ -SMA in 8-week MASH mice did not reach statistical significance when compared to 4-week MASH mice. Indeed, qRT-PCR analysis of *Acta2* (Fig. 3B) supported the finding from western blot results. Moreover, mRNA expression of *Col1a1* (Fig. 3C) was significantly elevated in both MASH mice groups compared to their respective control groups. However, no significant differences were observed between CDAA-fed animals at 4- and 8-weeks.

Sirius Red/Fast Green staining for the detection of collagen showed a

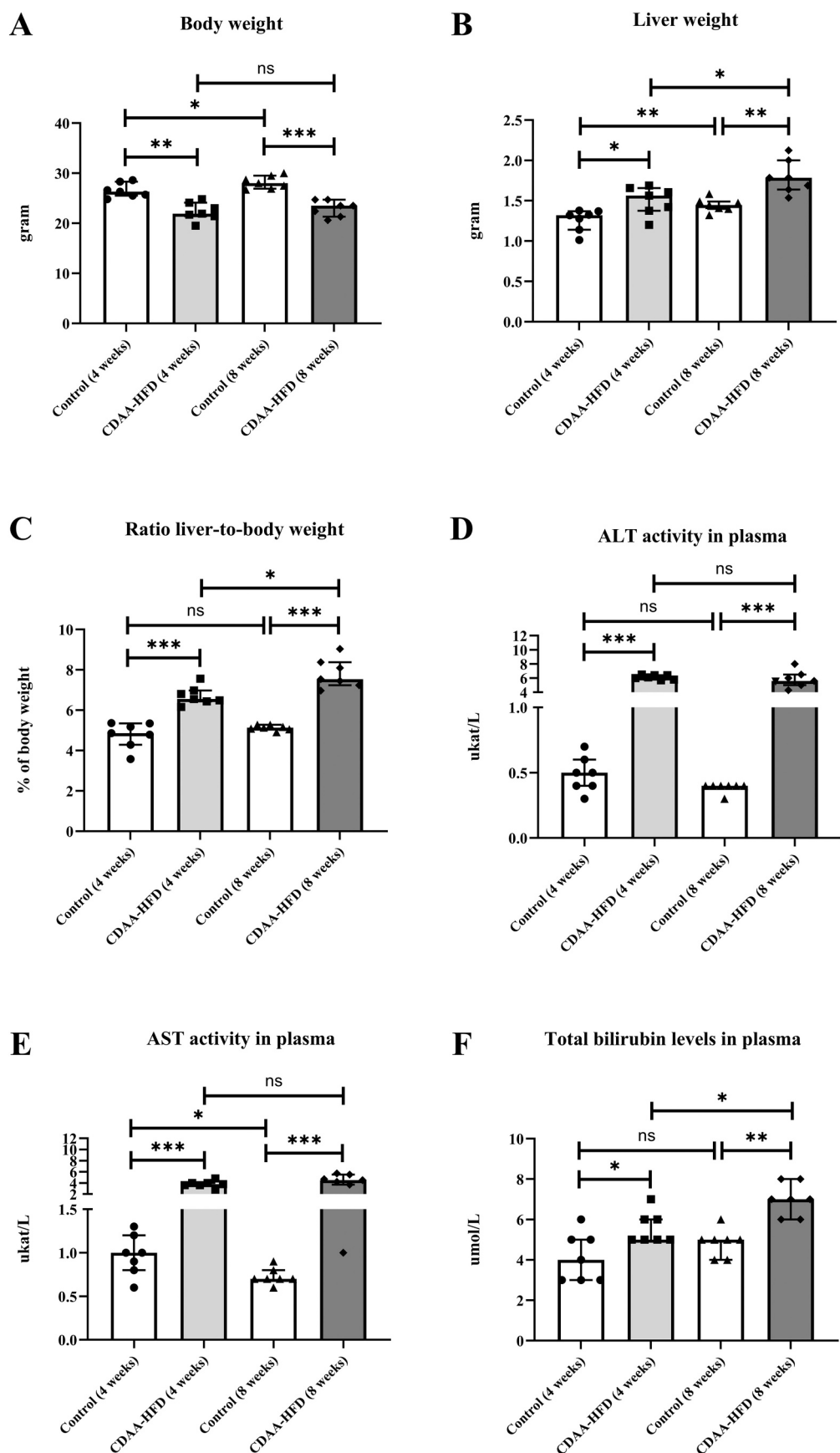
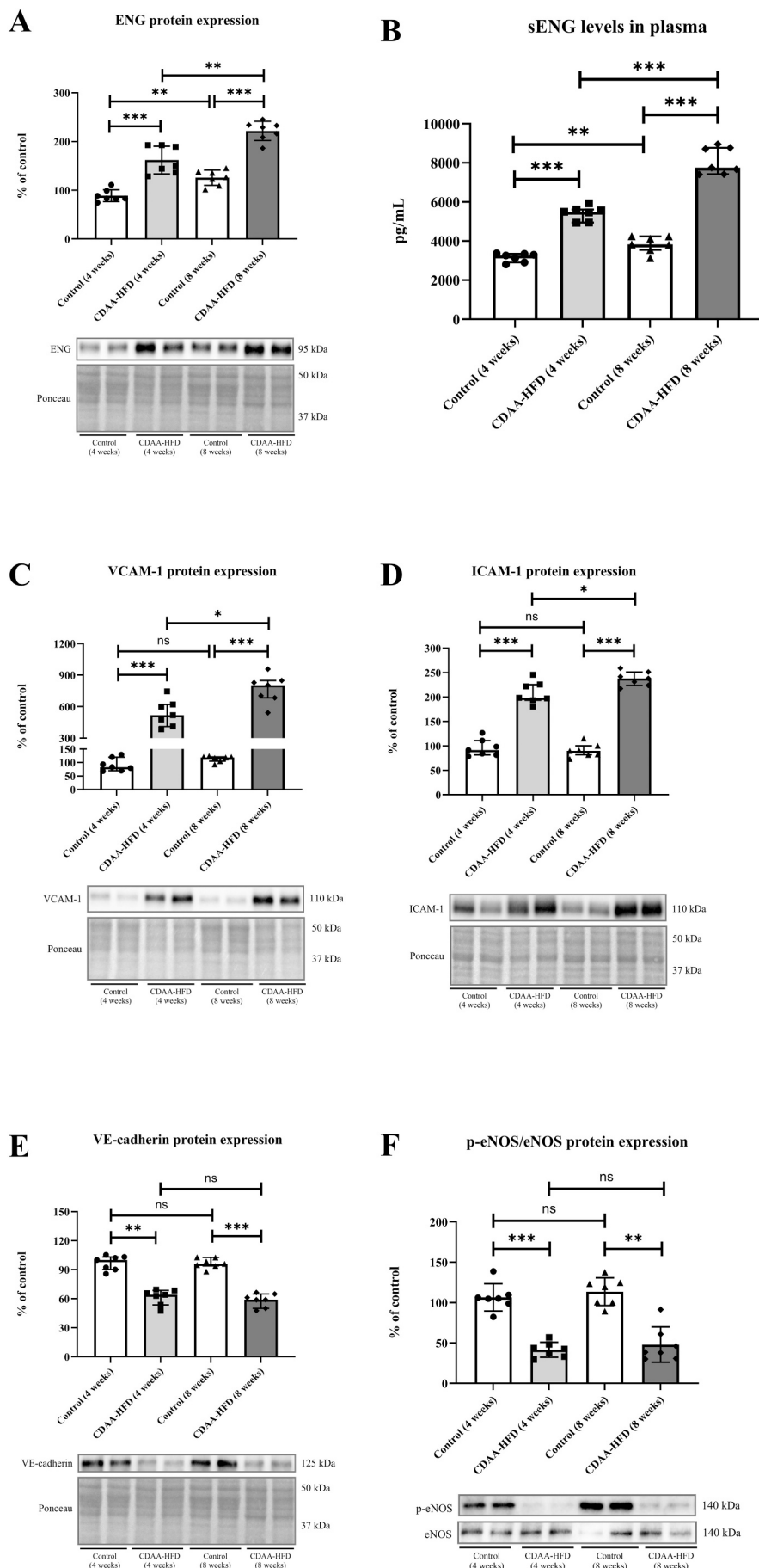


**Fig. 1.** Effect of a 4- and 8-week CDAA-HFD on liver parameters. Body weight (A), liver weight (B), and ratio liver-to-body weight (C). The activity of liver enzymes ALT (D) and AST (E) and total bilirubin levels (F) in plasma. Data are presented as median with interquartile range. Mann-Whitney test, ns (not significant), \*  $p < 0.05$ , \*\*  $p < 0.01$ , \*\*\*  $p < 0.001$ ; 7 animals per group.



(caption on next page)

**Fig. 2.** Biomarkers of sinusoidal endothelial inflammation/dysfunction in the liver. Protein expression of ENG (A) and sENG levels in plasma (B) measured by ELISA. Protein expression of VCAM-1 (C), ICAM-1 (D), VE-cadherin (E), and p-eNOS/eNOS (F). Data are presented as median with interquartile range. Mann-Whitney test, ns (not significant), \*  $p < 0.05$ , \*\*  $p < 0.01$ , \*\*\*  $p < 0.001$ ; 7 animals per group. Complete western blot results and Ponceau S staining are available in Supplementary Data 3.

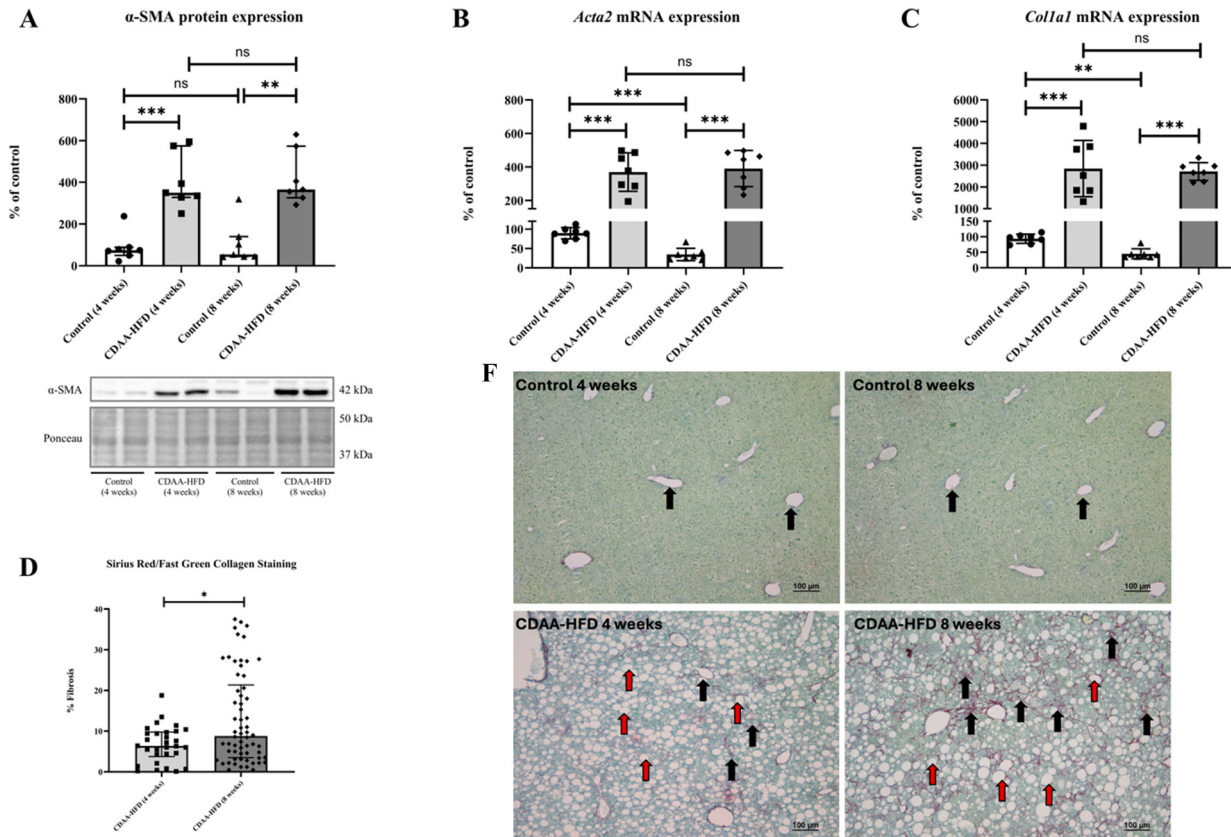


**Fig. 3.** Changes in liver fibrosis markers during MASH progression. Protein expression of  $\alpha$ -SMA (A), mRNA expression of *Acta2* (B), and *Col1a1* (C). Sirius Red/Fast Green quantification of fibrosis (D). Collagen (black arrows) and steatosis (red arrows) stained by Sirius Red/Fast Green in control liver and CDAA-HFD fed mice (E). Scale bar 100  $\mu$ m, 100 $\times$  magnification. Data are presented as median with interquartile range. Mann-Whitney test, ns (not significant), \*  $p < 0.05$ , \*\*  $p < 0.01$ , \*\*\*  $p < 0.001$ ; 7 animals per group. Complete western blot results of  $\alpha$ -SMA and Ponceau S staining are available in Supplementary Data 3.

reaction only in the wall of the central vein and the control group's arterioles and venules in the portal area (Fig. 3E). CDAA-HFD (both 4 and 8 weeks) resulted in liver steatosis and increased collagen deposition in liver periportal and perisinusoidal areas, suggesting the development of liver fibrosis. Interestingly, analysis of collagen deposition using Sirius Red staining showed a significantly higher level in 8-week-old mice (Fig. 3E), suggesting the progression of fibrosis and MASH, despite the fact that HSCs activation slowed down or reached a plateau after the initial 4 weeks in this particular MASH mouse model.

#### 3.4. The effect of M1043 antibody treatment on liver injury parameters in the MASH animal model

In this part of the study, we focused on the impact of the M1043 anti-ENG antibody on MASH progression.

Although our results did not show a significant effect of M1043 after a 4-week treatment on body weight (Fig. 4A) in MASH animal models, liver weight (Fig. 4 B), and the ratio of liver-to-body weight (Fig. 4C) were significantly decreased in M1043-treated animals compared to the IgG-injected group. The activity of ALT (Fig. 4D) and AST (Fig. 4E), as well as total bilirubin levels (Fig. 4F) in plasma, did not show statistical significance between IgG- and M1043-injected MASH mouse models.

#### 3.5. M1043 antibody treatment prevented the progression of MASH diet-induced LSECs inflammation in vivo

Although the mRNA expression of ENG (Fig. 5A) did not show any significant changes after M1043 treatment, it significantly prevented the increase in ENG protein expression (Fig. 5B) compared to IgG-injected mice, confirming a successful blocking effect of ENG following a 4-week treatment period. This is also supported by the fact that plasma levels of sENG (Fig. 5C) were significantly elevated in the MASH animal model treated with M1043 compared to both the control and MASH IgG-injected mice, suggesting that M1043 treatment may lead to shedding of membrane-bound ENG and its release into the bloodstream. This idea was supported by the detection of three distinct bands (approximately 65 kDa to 95 kDa) of ENG in the CDAA-HFD + M1043 group (Fig. 5C). Moreover, M1043 treatment significantly prevented p-SMAD1/5 (D) and ID1 (E) protein expression increase compared to IgG-injected MASH animals. This suggests that M1043 blockage affects BMP-9 binding to ENG and inhibits SMAD1/5/ID1 signaling.

Interestingly, protein expression of VCAM-1 (Fig. 5D) and ICAM-1 (Fig. 5E) increase was prevented in M1043-injected mice compared to those injected with IgG, suggesting a beneficial effect of M1043 in alleviating LSECs inflammation in MASH after a 4-week treatment period.

On the other hand, M1043 treatment did not significantly alter the

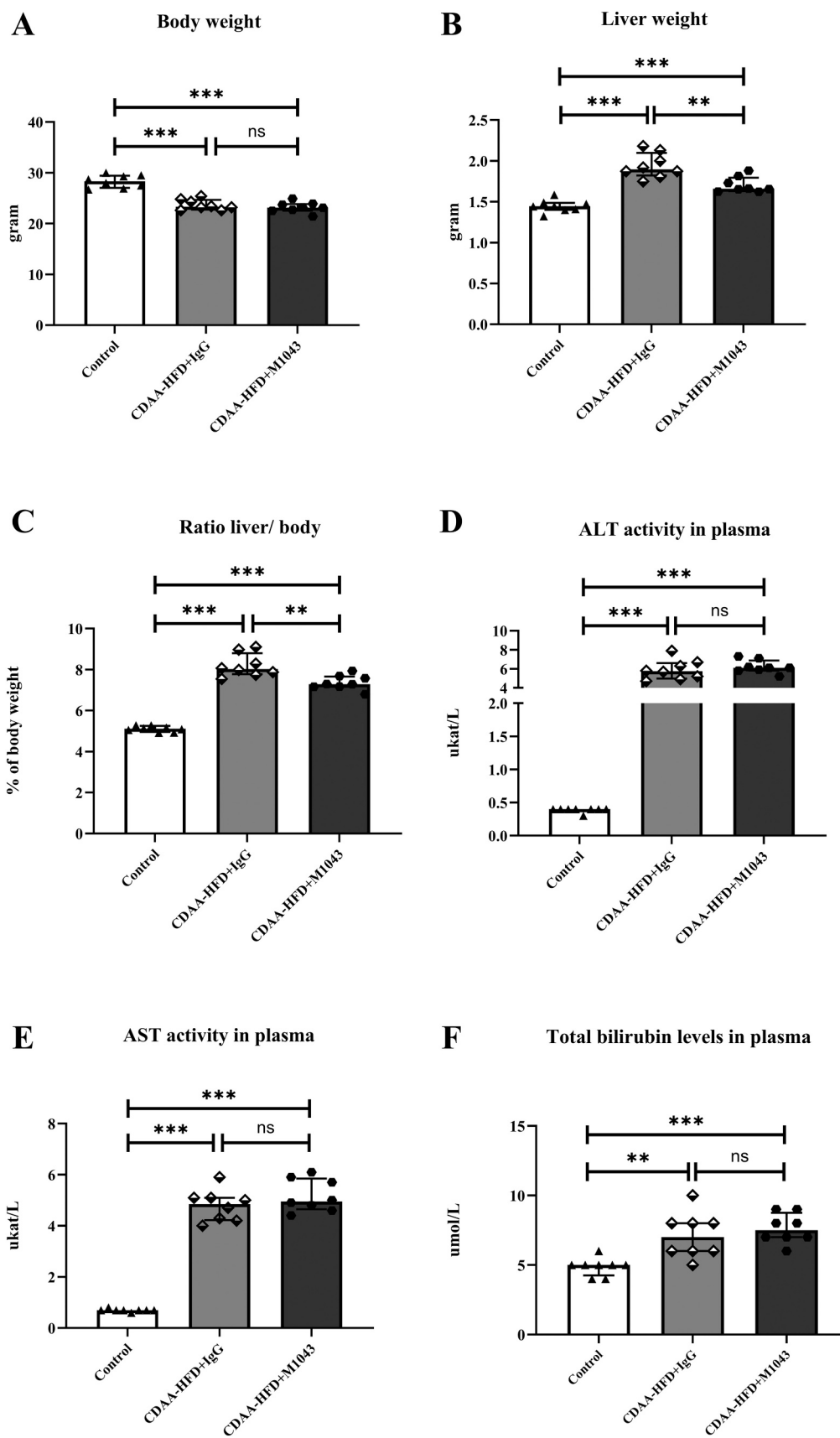


**Fig. 4.** M1043 effect on liver injury parameters in MASH mouse model. Body weight (A), liver weight (B), and ratio liver-to-body weight (C). The activity of liver enzymes (ALT) (D) and AST (E), and total bilirubin levels (F) in plasma. Data are presented as median with interquartile range. Mann-Whitney test, ns (not significant), \*\*  $p < 0.01$ , \*\*\*  $p < 0.001$ ; 8 animals per group.

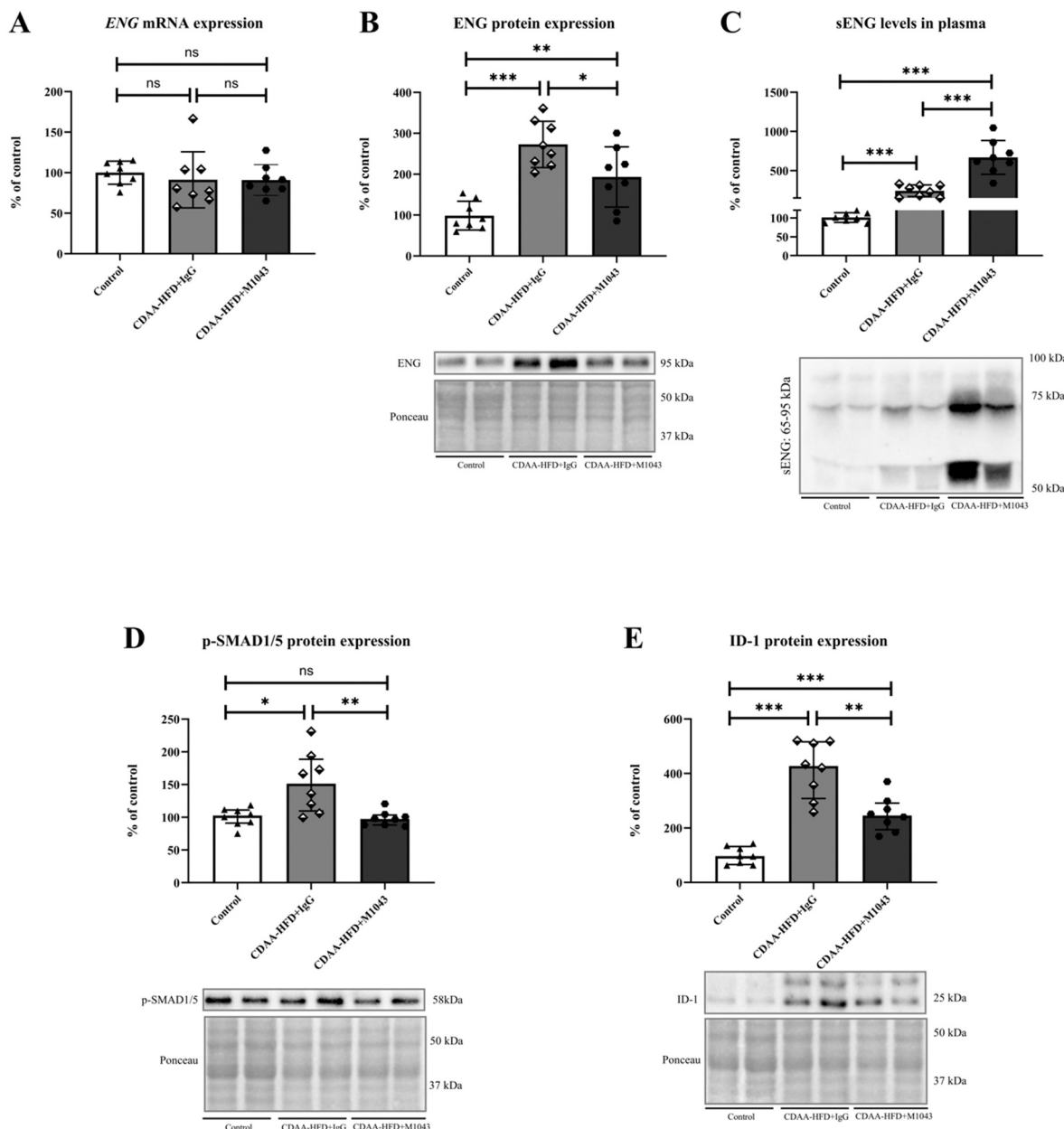


**Fig. 5.** Impact of M1043 treatment on LSED biomarkers in mouse models of MASH. mRNA expression of ENG (A), protein expression of ENG (B), and levels of sENG in plasma (C) were measured by western blot. Protein expression of p-SMAD1/5 (D), ID1 (E), VCAM-1 (F), ICAM-1 (G), VE-cadherin (H), and p-eNOS/eNOS (I). Data are presented as median with interquartile range. Mann-Whitney test, ns (not significant), \*  $p < 0.05$ , \*\*  $p < 0.01$ , \*\*\*  $p < 0.001$ ; 8 animals per group. Complete western blot results and Ponceau S staining are available in Supplementary Data 3. To confirm that rat IgG1 does not affect ENG protein expression in MASH mice, the western blot analysis is presented in Supplementary Data 4, comparing it with that of non-injected MASH animals.

protein expression of VE-cadherin (Fig. 5F) and p-eNOS/eNOS (Fig. 5G) compared to IgG-injected MASH mice.

### 3.6. TRC105 treatment prevents the development of LSECs inflammation *in vitro*

To find mechanistic details of the *in vivo* observation, we simulated the conditions induced by the CDAA-HFD mouse model in LSECs. Both mRNA and protein expression of ENG (Fig. 6A, F), VCAM-1 (Fig. 6D, H), and ICAM-1 (Fig. 6E, I) were significantly increased in LSECs induced by ox-LDL compared to the control group. Additionally, levels of sENG (Fig. 6G) were also significantly elevated. Due to ENG shedding induced by TRC105, two distinct bands (approximately 50 kDa to 100 kDa) of

ENG have been detected in the oxLDL+TRC105 group (Fig. 6G). All these changes indicate a successful induction of LSECs inflammation. Furthermore, these findings are supported by elevated mRNA levels of transcription factors regulating ENG protein levels (*RELA* (Fig. 6B) and *KLF6* (Fig. 6C)) and VCAM-1 and ICAM-1 protein levels (*RELA* (Fig. 6B)).

TRC105 treatment significantly reduced the ENG (Fig. 6F) and VCAM-1 (Fig. 6H) protein expression compared to both the control and ox-LDL groups, suggesting a potential effect of TRC105 on LSECs inflammation. Moreover, sENG levels (Fig. 6G) were significantly elevated after TRC105 treatment, suggesting the shedding of membrane-bound ENG and its release into the media. However, ICAM-1 protein expression did not reach statistical significance after TRC105 treatment (Fig. 6I).

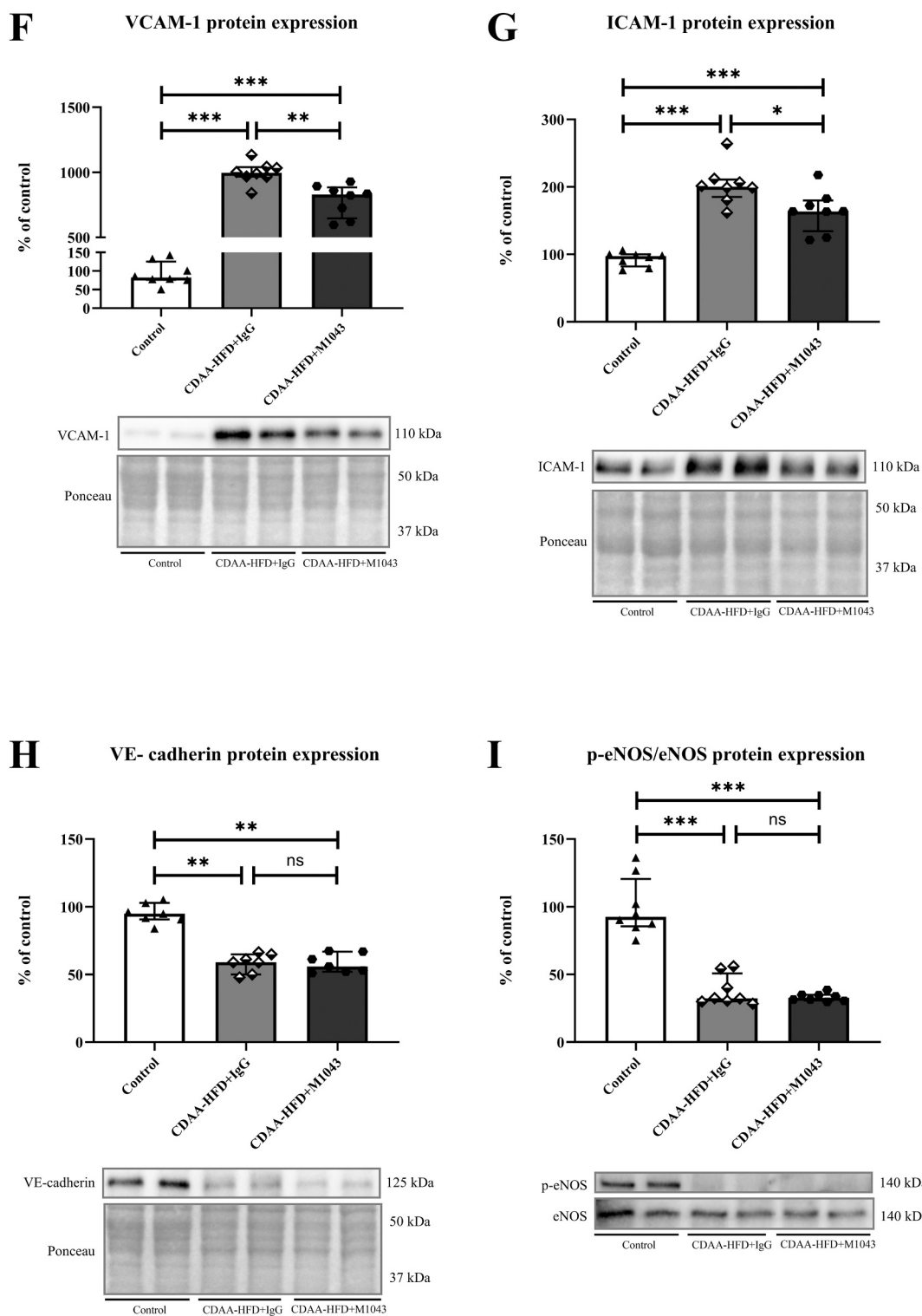
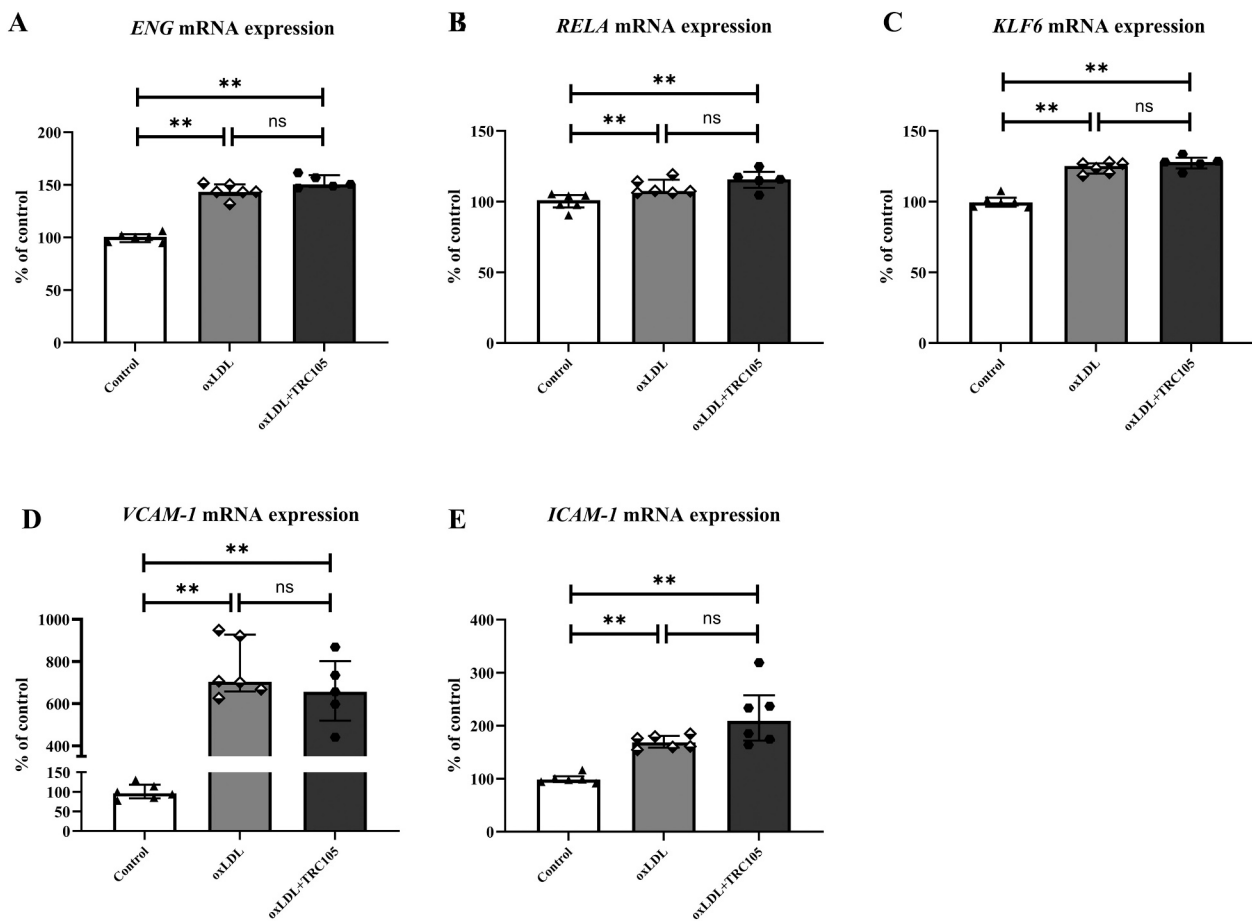


Fig. 5. (continued).

Additionally, ox-LDL induction significantly increased the adhesion of THP-1 monocytic cells to the endothelial monolayer compared to the control group, which was significantly reduced by TRC105 treatment (Fig. 6J), suggesting the potential effect of anti-ENG treatment on LSECs inflammation.

### 3.7. M1043 antibody treatment prevented the liver fibrosis progression in the MASH animal model

A significant increase in  $\alpha$ -SMA protein expression (Fig. 7A), *Acta2* mRNA expression (Fig. 7B), and mRNA expression of *Col1a1* (Fig. 7C) was observed in mice fed with the CDAA-HFD compared to the control groups. M1043 treatment did not significantly affect the protein expression of  $\alpha$ -SMA (Fig. 7A), *Acta2* mRNA expression (Fig. 7B), and



**Fig. 6.** Impact of TRC105 treatment on LSECs inflammation induced by ox-LDL in LSECs and THP-1 monocytic cell adhesion. mRNA expression of *ENG* (A), *RELA* (B), *KLF6* (C), *VCAM-1* (D), and *ICAM-1* (E) Protein expression of *ENG* (F) and sENG levels (G) were measured by western blot. Protein expression of *VCAM-1* (H) and *ICAM-1* (I). Number of adherent cells (J). Data are presented as median with interquartile range ( $n = 5-6$ , showing representative figures from 3 independent experiments). Mann-Whitney test, ns (not significant), \*  $p < 0.05$ , \*\*  $p < 0.01$ . The complete western blot result is available in Supplementary Data 3.

*Col1a1* mRNA expression (Fig. 7C). Despite that, M1043 treatment significantly prevented fibrosis progression compared to IgG-treated mice measured by Sirius Red/Fast Green staining (Fig. 7D, E).

#### 4. Discussion

In this study, we demonstrate for the first time that anti-*ENG* treatment with a monoclonal antibody prevents the progression of liver sinusoidal endothelial inflammation and fibrosis during MASH progression.

Our previous study showed that cholestatic liver injury and MASH lead to altered *ENG* expression, predominantly in LSECs. We suggested the importance of balanced physiological levels of *ENG* protein expression in LSECs for maintaining endothelial function [7]. However, the precise impact of potential anti-*ENG* treatment on LSECs inflammation and the development/progression of MASH has not been elucidated so far.

Thus, in this study, we hypothesized that blocking *ENG* with an anti-*ENG* antibody would prevent the progression LSECs inflammation and fibrosis during MASH development. In order to address this, we used the CDAA-HFD mouse model, which effectively induces rapid development of MASH-associated fibrosis [27].

Indeed, the CDAA-HFD diet resulted in liver impairment, as demonstrated by a higher liver-to-body weight ratio (indicating liver steatosis, hepatomegaly, inflammation, and fibrosis) and elevated liver enzyme activity (ALT and AST) and total bilirubin levels in plasma.

Additionally, liver weight, liver-to-body weight ratio, and total bilirubin levels significantly increased in 8-week MASH animals compared to those in 4-week MASH mice, whereas body weight and ALT, AST did not. In addition, we found fibrosis development after 4 weeks of the CDAA-HFD diet represented by increased expression of  $\alpha$ -SMA protein expression and *Acta*, *Col1a1* mRNA expression, and increased collagen deposition. Indeed, 8 weeks of diet administration resulted in fibrosis progression without further activation of HSCs. The induction of MASH in a mouse model using CDAA-HFD was previously reported in two separate studies, each involving feeding periods of 4 and 12 weeks [7,27]. Therefore, we propose a partial progression of liver impairment observed after eight weeks on the CDAA-HFD compared to the four-week induction.

However, in this study, we mainly focused on elucidating the role of *ENG* in the progression of LSECs inflammation and fibrosis in the MASH mouse model. The induction of MASH led to increased expression of *ENG*, predominantly in LSEC, as previously demonstrated in the same animal model [7]. These results were corroborated by Vicen et al. and Tripska et al., who established the essential role of *ENG* in ED triggered by 7-ketosterol and/or high glucose [10,23]. Moreover, *ENG* expression was significantly elevated in the 8-week MASH mice compared to the 4-week CDAA-HFD-fed mice in this study. Thus, we propose the potentially important role of *ENG* in promoting LSECs inflammation and fibrosis. These findings support the notion that *ENG* might be a key player in exacerbating LSECs inflammation and fibrosis, suggesting *ENG* as a promising target for potential therapeutic

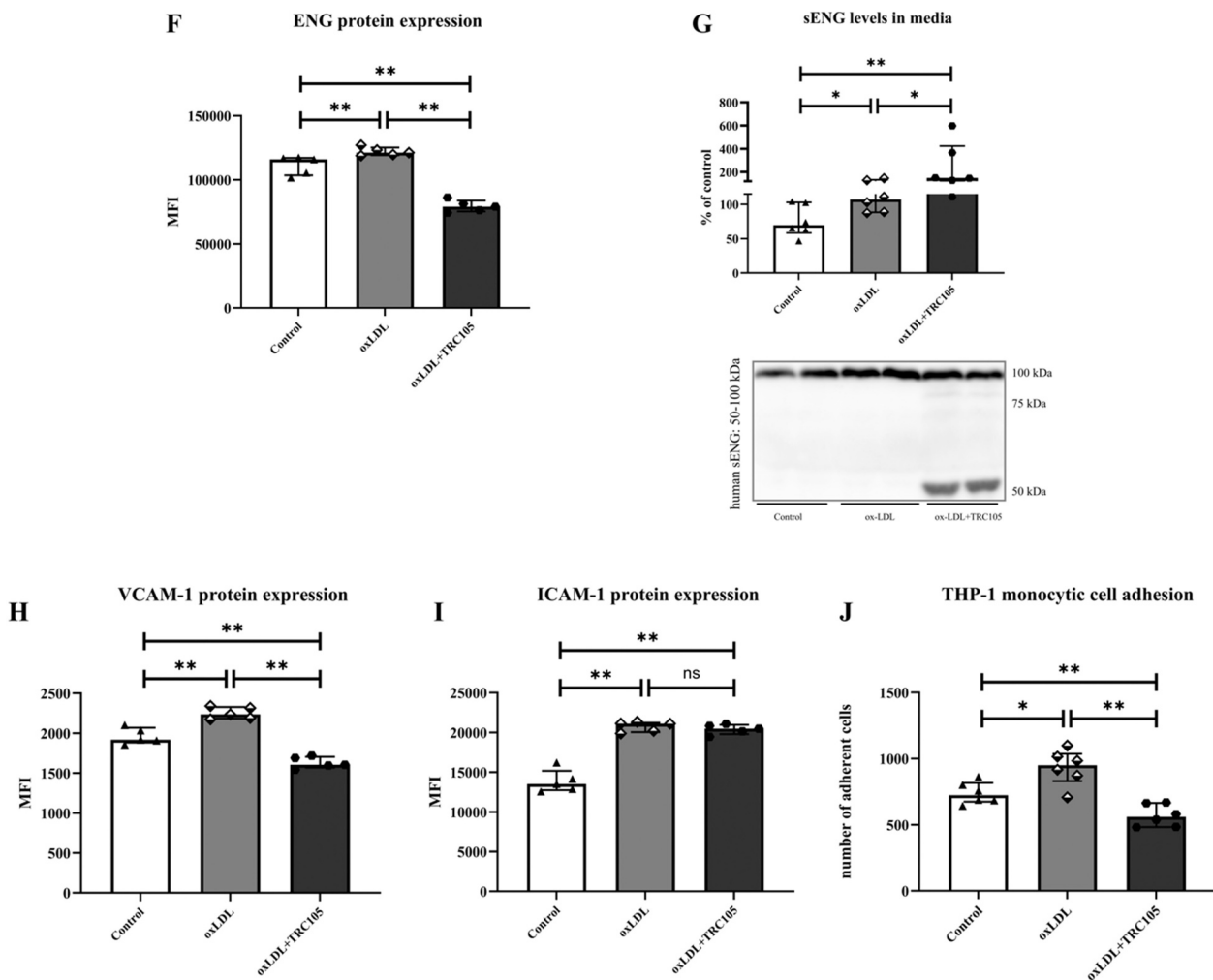


Fig. 6. (continued).

strategies, which we further explored in the next part of this study.

Elevated sENG levels in plasma have been detected in various pathological conditions associated with ED, such as atherosclerosis and type 2 diabetes mellitus [28–30], as well as different types of liver injury [7,8]. Consistent with these previous findings, we detected elevated sENG levels in the plasma of MASH mice, with a significant increase in the 8-week mice compared to the 4-week group. This suggests that the progression of liver impairment leads to further exacerbation of LSECs inflammation and fibrosis, as evidenced by the higher sENG levels in the more advanced stage of liver alteration, proposing the potential of sENG as a biomarker for monitoring the progression of LSECs inflammation and fibrosis in liver damage and emphasizing the importance of targeting ENG as a therapeutic strategy.

To further confirm the induction of LSECs inflammation, we analyzed the expression of VCAM-1 and ICAM-1. The elevated expression of these molecules promotes the infiltration of inflammatory cells into the liver, thereby contributing to the progression of liver impairment [31–33]. Indeed, we demonstrated previously that both VCAM-1 and ICAM-1 are predominantly expressed by LSECs, supporting the idea they are biomarkers of LSECs inflammation in this model [7]. The analysis revealed significant upregulation in the protein expression of both adhesion molecules in MASH mice compared to controls. Furthermore, their expression was notably higher in the 8-week MASH animals compared to those fed the CDAA-HFD for 4 weeks. These findings confirm LSECs inflammation over time in the MASH mouse model in this study.

In the second part of the study, we aimed to target ENG to affect LSECs inflammation and fibrosis in the MASH model using anti-ENG mAb. We used the M1043 antibody for *in vivo* experiments in mice [34] and TRC105 for *in vitro* study in human LSECs [10]. As demonstrated previously, both M1043 and TRC105 competitively inhibit BMP binding, preventing SMAD 1/5 phosphorylation [11].

The role of BMP-9 in liver alterations has been discussed previously, with some conflicting results. For instance, BMP-9 plays a critical role in vascular quiescence and is a key paracrine regulator controlling LSECs fenestration and protecting against perivascular hepatic fibrosis [35]. On the contrary, the important role of BMP-9/SMAD1/5/ID1 signaling as a profibrotic pathway in the liver has been demonstrated [35,36]. ID1 plays an important role in the transformation of HSCs into fibroblasts and in the epithelial-to-mesenchymal transition of HSCs [37]. Interestingly, it has been shown that ID1 activates the NF- $\kappa$ B signaling pathway through its physical and functional interaction with the p65 subunit [16], suggesting an impact on inflammation and the expression of VCAM-1, ICAM-1 [38]. Taken together, ID1 inhibition can be proposed as a target of the BMP-9//ENG/SMAD1/5 signaling pathway, which is associated with sinusoidal inflammation and fibrosis in the liver.

In this study, M1043 treatment prevented the increase of SMAD1/5/ID1 expression, suggesting that M1043 blockage affects the ENG/BMP9 interaction. Moreover, M1043 treatment prevented the increase of ENG, VCAM-1, and ICAM-1 in LSECs *in vivo*, suggesting reduced progression of LSECs inflammation in MASH mice, as LSECs predominantly express all these proteins in our study. In addition, M1043 treatment significantly

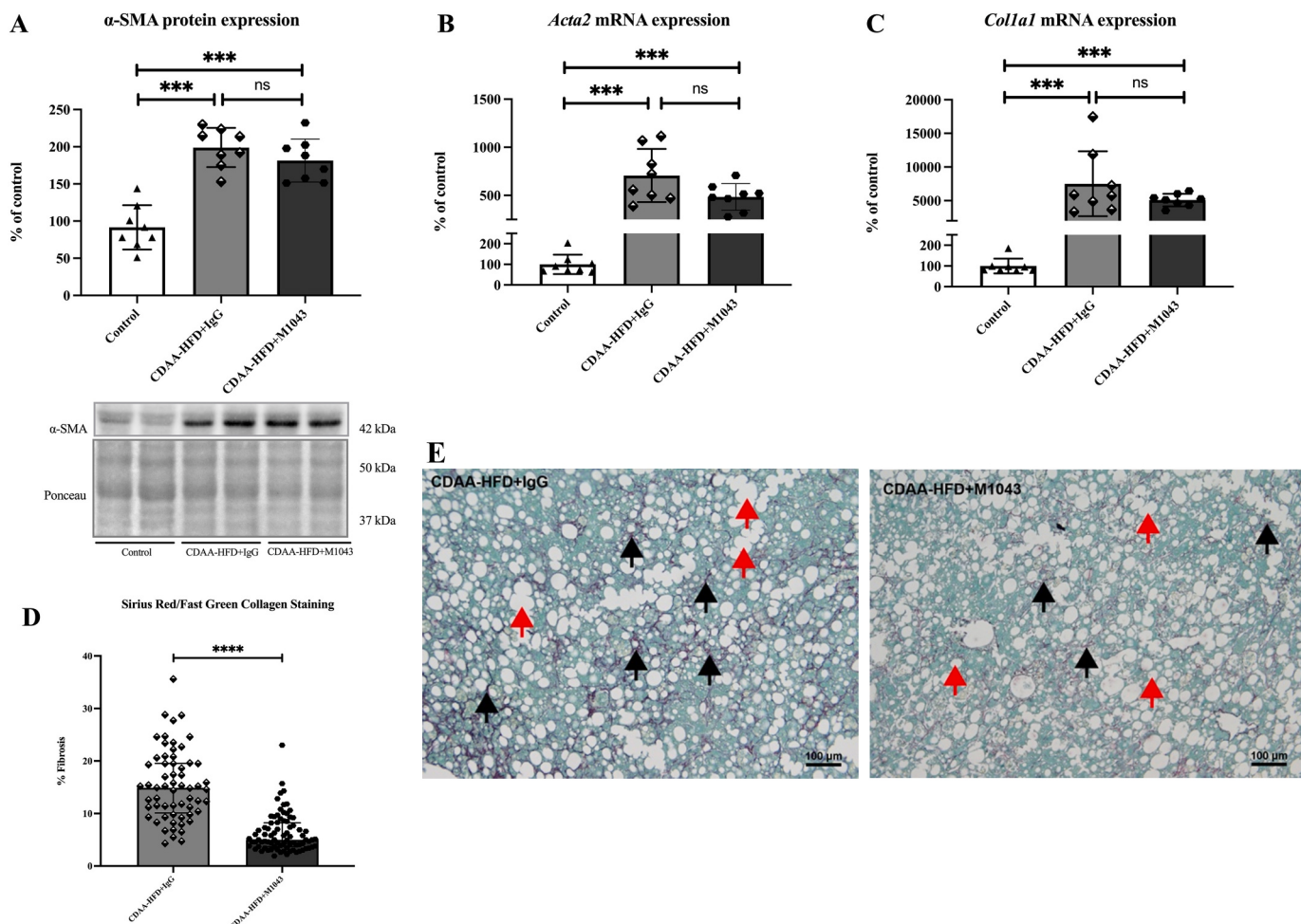


**Fig. 7.** M1043 treatment effects on fibrosis in a MASH animal model. Protein expression of  $\alpha$ -SMA (A), mRNA expression of *Acta2* (B), and *Colla1* (C). Sirius Red/Fast Green Collagen Staining (D). Collagen (black arrows) and steatosis (red arrows) stained by Sirius Red Fast Green in control liver and CDAA-HFD fed mice (D). Scale bar 100  $\mu$ m, 100 $\times$  magnification. Data are presented as median with interquartile range. Mann-Whitney test, ns (not significant), \*\*\*  $p < 0.001$ , \*\*\*\*  $p < 0.0001$ ; 8 animals per group. Complete Western blot results of  $\alpha$ -SMA and Ponceau S staining are available in Supplementary Data 3.

prevented liver fibrosis progression (collagen amount) and liver-to-body weight ratio (which reflects fibrosis as well), suggesting an antifibrotic effect of ENG blockage as well.

Thus, we propose that blocking the BMP-9/ENG/SMAD1 signaling cascade, including the SMAD1/5/ID1 pathway, with an anti-ENG antibody would prevent LSECs inflammation and fibrosis progression during MASH development.

Interestingly, M1043 and TRC105 treatment resulted in increased sENG levels without any significant changes in ENG gene expression, suggesting cleavage of ENG following treatment with both antibodies, as was shown previously [34]. This may be important for mitigating ENG-related effects on LSECs inflammation due to the fact that it has been demonstrated that sENG might antagonize ENG function in relation to adhesion, and transmigration of monocytes [9] and thrombus formation [39]. Moreover, high sENG levels are recognized as biomarker of MASH [7,8], and it is associated with MASH progression in this study. It is possible to suggest that the increased shedding of membrane-bound ENG may act as a defense mechanism by interfering with its role in the TGF- $\beta$  and integrin signaling pathways. Shedding of overexpressed membrane-bound ENG after treatment with M1043 and TRC105 could potentially disrupt the interaction between ENG and integrins, particularly  $\alpha$ 5 $\beta$ 1, as well as its involvement in TGF- $\beta$  signaling [40,41]. This disruption might contribute to mitigating ENG-mediated inflammatory and fibrotic signaling, as indicated by reduced LSECs inflammation and fibrosis in MASH models and decreased inflammation in human LSECs *in vitro*.

However, the precise mechanisms underlying the increase in sENG after M1043 and TRC105 treatment remain to be further elucidated, and additional studies are required to fully clarify these effects.

In addition, we aimed to determine whether human LSECs in *in vitro* conditions can mimic the LSECs inflammation observed in the *in vivo* study. Ox-LDL treatment induced mRNA expression of *ENG* and respective transcription factors (*RELA*, *KLF6*) accountable for regulating ENG protein expression, as shown previously [10,23]. Moreover, we demonstrated that TRC105 prevented the increase in ENG and VCAM-1 protein expression and reduced THP-1 monocytic cells adhesion to the endothelium, suggesting reduced LSEC inflammation as demonstrated *in vivo*. It is noteworthy that preventing ENG overexpression through antibody treatment may reduce monocyte adhesion to the endothelium, as ENG interacts with the  $\alpha$ 5 $\beta$ 1 integrin, a fibronectin receptor abundantly expressed on most leukocyte populations, including lymphocytes, monocytes, and granulocytes [42,43].

## 5. Conclusion

In conclusion, we demonstrate for the first time that anti-ENG antibody treatment can prevent LSECs inflammation and fibrosis in a MASH animal model, as well as reduce inflammation in LSECs *in vitro*. We propose that targeting ENG might represent an interesting pharmacological approach concerning LSECs inflammation and fibrosis in MASH.

## CRediT authorship contribution statement

**Samira Eissazadeh:** Writing – review & editing, Writing – original draft, Methodology, Investigation, Formal analysis, Data curation. **Petra Fikrova:** Writing – review & editing, Writing – original draft, Methodology, Investigation, Formal analysis, Data curation. **Jana Urbankova Rathouska:** Writing – review & editing, Methodology. **Ivana Nemecova:** Writing – review & editing, Methodology. **Katarina Tripska:** Writing – review & editing, Methodology. **Martina Vasinova:** Writing – review & editing, Methodology. **Radim Havelek:** Methodology, Data curation. **SeyedehNiloufar Mohammadi:** Writing – review & editing, Methodology. **Ivone Cristina Igreja Sa:** Writing – review & editing, Methodology. **Charles Theuer:** Writing – review & editing. **Matthias König:** Writing – review & editing. **Stanislav Micuda:** Writing – review & editing, Writing – original draft, Funding acquisition. **Petr Nachtigal:** Writing – review & editing, Writing – original draft, Supervision, Project administration, Funding acquisition, Conceptualization.

## Consent for publication

Not applicable.

## Ethics approval and consent to participate

Not applicable.

## Funding

This research was supported by grants from the Czech Science Foundation [GACR No. 22-14961S], the Grant Agency of Charles University [GAUK No. 362221], Specific University Research [SVV 260 663], The project New Technologies for Translational Research in Pharmaceutical Sciences /NETPHARM, project ID CZ.02.01.01/00/22\_008/0004607, is co-funded by the European Union. MK was supported by the German Research Foundation (DFG) by grant numbers 436883643 and 465194077 and by the Federal Ministry of Education and Research (BMBF, Germany) by grant number 031L0304B.

## Declaration of competing interest

Dr. Theurer is the former CEO and president of Tracon Pharmaceuticals, Inc. The remaining authors declare that the research was conducted without any commercial or financial relationships that could be recognized as potential conflicts of interest.

## Acknowledgments

We wish to express our sincere appreciation to Prof. Lukas Hawinkels from the Department of Gastroenterology and Hepatology, Leiden University Medical Center, Leiden, the Netherlands, for his generosity in providing rat IgG1 and M1043. Your invaluable contributions have been crucial to the success of our research. We sincerely thank Dr. Sona Kauerova from the Institute for Clinical and Experimental Medicine, Prague, Czech Republic, for generously providing the THP-1 cell line. We thank the Department of Medical Biochemistry, Faculty of Medicine in Hradec Králové, for providing us with their equipment and resources. We are particularly grateful to Dr. Milos Hroch, M.Sc. Mohammedreza Afshari and Dr. Eva Petrova for their invaluable assistance and support throughout this study. Their expertise and dedication have contributed significantly to the success of our research.

## Appendix A. Supplementary data

Supplementary data to this article can be found online at <https://doi.org/10.1016/j.lfs.2025.123428>.

## Data availability

The original contributions of this study are detailed in the article; further inquiries can be directed to the corresponding author.

## References

- [1] J. Poisson, S. Lemoinne, C. Boulanger, F. Durand, R. Moreau, D. Valla, P.-E. Rautou, Liver sinusoidal endothelial cells: physiology and role in liver diseases, *J. Hepatol.* 66 (2017) 212–227.
- [2] A. Hammouette, P.-E. Rautou, Role of liver sinusoidal endothelial cells in non-alcoholic fatty liver disease, *J. Hepatol.* 70 (2019) 1278–1291.
- [3] A.L. Wilkinson, M. Qurashi, S. Shetty, The role of sinusoidal endothelial cells in the axis of inflammation and cancer within the liver, *Front. Physiol.* 11 (2020) 990.
- [4] J. Gracia-Sanche, E. Caparrós, A. Fernández-Iglesias, R. Francés, Role of liver sinusoidal endothelial cells in liver diseases, *Nat. Rev. Gastroenterol. Hepatol.* 18 (2021) 411–431.
- [5] E. Lafoz, M. Ruart, A. Anton, A. Oncins, V. Hernández-Gea, The endothelium as a driver of liver fibrosis and regeneration, *Cells* 9 (2020) 929.
- [6] L.D. Deleve, X. Wang, Y. Guo, Sinusoidal endothelial cells prevent rat stellate cell activation and promote reversion to quiescence, *Hepatology* 48 (2008) 920–930.
- [7] S. Eissazadeh, S. Mohammadi, F.A. Faradonbeh, J.U. Rathouska, I. Nemeckova, K. Tripska, B. Vitverova, E. Dohnálkova, M. Vasinova, P. Fikrova, I.C.J. Sa, S. Micuda, P. Nachtigal, Endoglin and soluble endoglin in liver sinusoidal endothelial dysfunction in vivo, *Biochim. Biophys. Acta Mol. basis Dis.* 1870 (2024) 166990.
- [8] I.C. Igreja Sa, K. Tripska, M. Hroch, R. Hyspler, A. Ticha, H. Lastuvkova, J. Schreiberova, E. Dolezelova, S. Eissazadeh, B. Vitverova, I. Najmanova, M. Vasinova, M. Pericacho, S. Micuda, P. Nachtigal, Soluble Endoglin as a Potential Biomarker of Nonalcoholic Steatohepatitis (NASH) Development, Participating in Aggravation of NASH-Related Changes in Mouse Liver, 2020 (Int J Mol Sci 21).
- [9] E. Rossi, F. Sanz-Rodriguez, N. Eleno, A. Duwell, F.J. Blanco, C. Langa, L. M. Botella, C. Cabanas, J.M. Lopez-Novoa, C. Bernabeu, Endothelial endoglin is involved in inflammation: role in leukocyte adhesion and transmigration, *Blood* 121 (2013) 403–415.
- [10] K. Tripska, I.C. Igreja Sa, M. Vasinova, M. Vicen, R. Havelek, S. Eissazadeh, Z. Svobodova, B. Vitverova, C. Bernabeu, P. Nachtigal, Monoclonal anti-endoglin antibody TRC105 (carotuximab) prevents hypercholesterolemia and hyperglycemia-induced endothelial dysfunction in human aortic endothelial cells, *Front Med (Lausanne)* 9 (2012) 845918.
- [11] O. Nolan-Stevaux, W. Zhong, S. Culp, K. Shaffer, J. Hoover, D. Wickramasinghe, A. Rueffli-Brasse, Endoglin requirement for BMP9 signaling in endothelial cells reveals new mechanism of action for selective anti-endoglin antibodies, *PLoS One* 7 (2012) e50920.
- [12] Y. Liu, H. Tian, G.C. Blobe, C.P. Theuer, H.I. Hurwitz, A.B. Nixon, Effects of the combination of TRC105 and bevacizumab on endothelial cell biology, *Investig. New Drugs* 32 (2014) 851–859.
- [13] Y. Liu, M.D. Starr, J.C. Brady, A. Dellinger, H. Pang, B. Adams, C.P. Theuer, N. Y. Lee, H.I. Hurwitz, A.B. Nixon, Modulation of circulating protein biomarkers following TRC105 (anti-endoglin antibody) treatment in patients with advanced cancer, *Cancer Med.* 3 (2014) 580–591.
- [14] L.S. Rosen, H.I. Hurwitz, M.K. Wong, J. Goldman, D.S. Mendelson, W.D. Figg, S. Spencer, B.J. Adams, D. Alvarez, B.K. Seon, C.P. Theuer, B.R. Leigh, M. S. Gordon, A phase I first-in-human study of TRC105 (anti-Endoglin antibody) in patients with advanced cancer, *Clin. Cancer Res.* 18 (2012) 4820–4829.
- [15] J.M. Munoz-Felix, M. Gonzalez-Nunez, J.M. Lopez-Novoa, ALK1-Smad1/5 signaling pathway in fibrosis development: friend or foe? *Cytokine Growth Factor Rev.* 24 (2013) 523–537.
- [16] X. Peng, Y. Wang, S. Kolli, J. Deng, L. Li, Z. Wang, J.U. Raj, D. Gou, Physical and functional interaction between the ID1 and p65 for activation of NF-κappaB, *Am. J. Phys. Cell Physiol.* 303 (2012) C267–C277.
- [17] S. Shetty, P.F. Lalor, D.H. Adams, Liver sinusoidal endothelial cells—gatekeepers of hepatic immunity, *Nat. Rev. Gastroenterol. Hepatol.* 15 (2018) 555–567.
- [18] Q. Guo, K. Furuta, S. Islam, N. Caporarello, E. Kostallari, K. Dielis, D. J. Tschumperlin, P. Hirsova, S.H. Ibrahim, Liver sinusoidal endothelial cell expressed vascular cell adhesion molecule 1 promotes liver fibrosis, *Front. Immunol.* 13 (2022) 983255.
- [19] A. Benedicto, A. Herrero, I. Romayor, J. Marquez, B. Smedsrød, E. Olaso, B. Arteta, Liver sinusoidal endothelial cell ICAM-1 mediated tumor/endothelial crosstalk drives the development of liver metastasis by initiating inflammatory and angiogenic responses, *Sci. Rep.* 9 (2019) 13111.
- [20] D. Vestweber, VE-cadherin: the major endothelial adhesion molecule controlling cellular junctions and blood vessel formation, *Arterioscler. Thromb. Vasc. Biol.* 28 (2008) 223–232.
- [21] M. Siragusa, I. Fleming, The eNOS signalosome and its link to endothelial dysfunction, *Pflügers Archiv-European Journal of Physiology* 468 (2016) 1125–1137.
- [22] R. Wakasugi, K. Suzuki, T. Kaneko-Kawano, Molecular mechanisms regulating vascular endothelial permeability, *Int. J. Mol. Sci.* 25 (2024).
- [23] M. Vicen, B. Vitverova, R. Havelek, K. Blazickova, M. Machacek, J. Rathouska, I. Najmanova, E. Dolezelova, A. Prasnicka, M. Sternak, C. Bernabeu, P. Nachtigal, Regulation and role of endoglin in cholesterol-induced endothelial and vascular dysfunction in vivo and in vitro, *FASEB J.* 33 (2019) 6099–6114.

- [24] M.L. Graham, M.J. Prescott, The multifactorial role of the 3Rs in shifting the harm-benefit analysis in animal models of disease, *Eur. J. Pharmacol.* 759 (2015) 19–29.
- [25] A. Prasnicka, J. Germanova, M. Hroch, E. Dolezelova, L. Rozkydalova, T. Smutny, A. Carazo, J. Chladek, M. Lenicek, P. Nachtigal, Iron depletion induces hepatic secretion of biliary lipids and glutathione in rats, *Biochimica et Biophysica Acta (BBA)-molecular and cell biology of Lipids* 1862 (2017) 1469–1480.
- [26] P. Nachtigal, V. Semecky, M. Kopecky, A. Gojova, D. Solichova, P. Zdansky, Z. Zadak, Application of stereological methods for the quantification of VCAM-1 and ICAM-1 expression in early stages of rabbit atherogenesis, *Pathol. Res. Pract.* 200 (2004) 219–229.
- [27] M. Matsumoto, N. Hada, Y. Sakamaki, A. Uno, T. Shiga, C. Tanaka, T. Ito, A. Katsume, M. Sudoh, An improved mouse model that rapidly develops fibrosis in non-alcoholic steatohepatitis, *Int. J. Exp. Pathol.* 94 (2013) 93–103.
- [28] E. Fonsatti, L.D. Vecchio, M. Altomonte, L. Sigalotti, M.R. Nicotra, S. Coral, P. G. Natali, M. Maio, Endoglin: an accessory component of the TGF- $\beta$ -binding receptor-complex with diagnostic, prognostic, and bioimmunotherapeutic potential in human malignancies, *J. Cell. Physiol.* 188 (2001) 1–7.
- [29] M. Varejckova, E. Gallardo-Vara, M. Vicen, B. Vitverova, P. Fikrova, E. Dolezelova, J. Rathouska, A. Prasnicka, K. Blazickova, S. Micuda, Soluble endoglin modulates the pro-inflammatory mediators NF- $\kappa$ B and IL-6 in cultured human endothelial cells, *Life Sci.* 175 (2017) 52–60.
- [30] B. Vitverova, K. Blazickova, I. Najmanova, M. Vicen, R. Hyšpler, E. Dolezelova, I. Nemeckova, J.D. Tebbens, C. Bernabeu, M. Pericacho, Soluble endoglin and hypercholesterolemia aggravate endothelial and vessel wall dysfunction in mouse aorta, *Atherosclerosis* 271 (2018) 15–25.
- [31] R.M. Carr, VCAM-1: closing the gap between lipotoxicity and endothelial dysfunction in nonalcoholic steatohepatitis, *J. Clin. Invest.* 131 (2021).
- [32] K.-J. Chung, A.-I. Legaki, G. Papadopoulos, B. Gercken, J. Gebler, R.F. Schwabe, T. Chavakis, A. Chatzigeorgiou, Analysis of the role of stellate cell VCAM-1 in NASH models in mice, *Int. J. Mol. Sci.* 24 (2023) 4813.
- [33] R.-I. Velliou, A.-I. Legaki, P. Nikolakopoulou, N.I. Vlachogiannis, A. Chatzigeorgiou, Liver endothelial cells in NAFLD and transition to NASH and HCC, *Cell. Mol. Life Sci.* 80 (2023) 314.
- [34] M.J.A. Schoonderwoerd, M.F.M. Koops, R.A. Angela, B. Koolmoes, M. Toitou, M. Paauwe, M.C. Barnhoorn, Y. Liu, C.F.M. Sier, J.C.H. Hardwick, A.B. Nixon, C. P. Theuer, M.F. Fransen, L. Hawinkels, Targeting Endoglin-expressing regulatory T cells in the tumor microenvironment enhances the effect of PD1 checkpoint inhibitor immunotherapy, *Clin. Cancer Res.* 26 (2020) 3831–3842.
- [35] A. Desroches-Castan, E. Tillet, N. Ricard, M. Ouarne, C. Mallet, L. Belmudes, Y. Coute, O. Boillot, J.Y. Scoazec, S. Bailly, J.J. Feige, Bone morphogenetic protein 9 is a paracrine factor controlling liver sinusoidal endothelial cell fenestration and protecting against hepatic fibrosis, *Hepatology* 70 (2019) 1392–1408.
- [36] K. Breitkopf-Heinlein, C. Meyer, C. Konig, H. Gaitantri, A. Addante, M. Thomas, E. Wiercinska, C. Cai, Q. Li, F. Wan, C. Hellerbrand, N.A. Valous, M. Hahnel, C. Ehling, J.G. Bode, S. Muller-Bohl, U. Klingmuller, J. Altenoder, I. Ilkavets, M. J. Goumans, L.J. Hawinkels, S.J. Lee, M. Wieland, C. Mogler, M.P. Ebert, B. Herrera, H. Augustin, A. Sanchez, S. Dooley, P. Ten Dijke, BMP-9 interferes with liver regeneration and promotes liver fibrosis, *Gut* 66 (2017) 939–954.
- [37] J. Bi, S. Ge, Potential roles of BMP9 in liver fibrosis, *Int. J. Mol. Sci.* 15 (2014) 20656–20667.
- [38] K. Ley, Y. Huo, VCAM-1 is critical in atherosclerosis, *J. Clin. Invest.* 107 (2001) 1209–1210.
- [39] E. Rossi, M. Pericacho, A. Kauskot, L. Gamella-Pozuelo, E. Reboul, A. Leuci, C. Egido-Turrión, D. El Hamaoui, A. Marchelli, F.J. Fernandez, I. Margall, M. C. Vega, P. Gaussem, S. Pasquali, D.M. Smadja, C. Bachet-Loza, C. Bernabeu, Soluble endoglin reduces thrombus formation and platelet aggregation via interaction with alphaiIbbeta3 integrin, *J. Thromb. Haemost.* 21 (2023) 1943–1956.
- [40] N.Y. Lee, B. Ray, T. How, G.C. Blobe, Endoglin promotes transforming growth factor beta-mediated Smad 1/5/8 signaling and inhibits endothelial cell migration through its association with GIPC, *J. Biol. Chem.* 283 (2008) 32527–32533.
- [41] H. Tian, K. Mythreya, C. Golzio, N. Katsanis, G.C. Blobe, Endoglin mediates fibronectin/alpha5beta1 integrin and TGF-beta pathway crosstalk in endothelial cells, *EMBO J.* 31 (2012) 3885–3900.
- [42] E. Rossi, C. Bernabeu, Novel vascular roles of human endoglin in pathophysiology, *J. Thromb. Haemost.* 21 (2023) 2327–2338.
- [43] K. Ley, C. Laudanna, M.I. Cybulsky, S. Nourshargh, Getting to the site of inflammation: the leukocyte adhesion cascade updated, *Nat. Rev. Immunol.* 7 (2007) 678–689.